Exploring controls on perfluorocarboxylic acid (PFCA) gas-particle partitioning using a model with observational constraints

Ye Tao [1], Trevor C. VandenBoer [1], RenXi Ye[1], Cora J. Young *[1]

1. Department of Chemistry, York University, Toronto, Ontario, Canada

* Corresponding author: youngcj@yorku.ca

Abstract. The atmospheric fate of perfluorocarboxylic acids (PFCAs) has attracted much attention in recent decades due to the role of the atmosphere in global transport of these persistent chemicals. There is a gap in our understanding of gas-particle partitioning, limited by availability of reliable atmospheric measurements, partitioning properties, and models of gas-particle interactions. The gas-particle equilibrium phase partitioning of C2-C16 PFCAs in the atmosphere were modeled here by taking account of both deprotonation and phase partitioning equilibria among air, aerosol liquid water, and particulate water-insoluble organic matter using a range of available PFCA partitioning properties. We systematically varied water and organic matter content to simulate the full range of atmospheric conditions. Except in severe organic matter pollution episodes, shorter-chain PFCAs are predicted to mainly partition between air and aqueous phase, while for PFCAs with carbon chains longer than 12, organic matter is more likely to be the dominant particle phase reservoir. The model framework underestimated the particle fraction of C2-C8 PFCAs compared with several ambient observations, with larger discrepancies observed for longer-chain PFCAs. The discrepancy could result from externally mixed dust components, non-ideality of aerosol liquid water, surfactant descriptions at phase boundaries, and missed interactions between organic matter and charged PFCA molecules. Reliable measurements of ambient PFCAs with high time

resolution and the measurement of uptake parameters by particle-relevant components will be beneficial to more reliable environmental fate modeling of ambient PFCAs.

Key words: PFCAs, PFAS, gas-particle partitioning, thermodynamic modeling, aerosol

Environmental Significance:

Perfluorocarboxylic acids (PFCAs) are widely used in commercial products, but are globally distributed, persistent, and some are toxic to humans and wildlife. A mechanistic understanding of the atmospheric fate and transport of PFCAs is crucial to reliably predict PFCA spatial and temporal distribution. In this study, we modeled the gas-particle partitioning of multiple PFCAs under a wide range of realistic atmospheric conditions and compared these with several reliable observational studies. Significant discrepancies were identified between modeling and observation results, particularly for longer-chain PFCAs, which suggests missing mechanisms. We conclude that there is a necessity to increase the number of reliable high time-resolution observations and laboratory phase partitioning studies.

1. Introduction

Poly- and perfluoroalkyl substances (PFAS) have been manufactured and widely used for commercial products due to their excellent chemical and thermal stabilities.[1,2] Perfluorocarboxylic acids (PFCAs) are a sub-group of PFAS that are important to understand because they are persistent, bioaccumulative, and found globally, far from areas in which they are produced or used.[3–7] PFCAs with chain lengths ranging from two carbon atoms (C2) to more than fourteen carbon atoms (C14) have been measured in the atmosphere.[8–10] Prior studies have established that a major contributor to global distribution of PFCAs is atmospheric formation and transport.[11–13] Atmospheric PFCA transport can occur through the gas or aerosol phase; however, the extent of transport depends on whether they are found in gas or aerosol.[14,15] Thus, a mechanistic understanding using relevant atmospheric chemistry conditions

and parameters is necessary to include gas-particle partitioning in global chemical transport models, where it has sometimes been excluded (e.g., [12]).

Atmospheric aerosol is a complex mixture of inorganic salts, water-soluble organic matter, water-insoluble organic matter, and a wide variety of other compounds.[16] Depending on chemical composition and meteorological conditions, aerosol can have phase separated water-insoluble organic and aqueous phases that can impact the partitioning of organic matter and water-soluble molecules of interest, respectively.[17,18] Considering that the pH values of aerosol liquid water can range from -1 to 5, and cloud or fog droplets from 2-7,[19] factors influencing the acidity of atmospheric liquid water can also significantly impact the transportation characteristics of PFCAs. To our knowledge, only a single laboratory experiment has been conducted to understand gas-particle partitioning of PFCAs, which exposed filter-collected ambient aerosols to C6, C7, and C8 gaseous PFCAs at levels orders of magnitude above those that are relevant in the atmosphere to facilitate detection of the PFCAs.[20] Most attempts to understand gas-particle partitioning of PFCAs have been through simultaneous gas and particle measurements integrated over several hours to days (e.g., [8,15,21–24]). However, about half of the studies that have examined gas-particle partitioning of PFCAs with chain lengths ≥4 have relied upon the collection of particles prior to gases (e.g., in high volume air samplers[21,22,24]). Sampling in this way is well established to lead to artifacts for long-studied atmospheric acids like HNO_3,[25–27] and has been shown to cause blow-on effects and an over-estimate of PFCAs in the particle phase.[28–30] For example, Ahrens et al.[29] found that high volume air samplers can severely overestimate the particle phase fraction of PFCAs by more than 60 % for C8-C12 PFCAs compared to a denuder sampler followed by a particle filter. This suggests that, like other atmospheric acids, accurate quantification of gaseous and particulate PFCAs requires collection of the gas phase prior to the particles[31] or collecting both phases simultaneously.[32] Several studies have used reliable methods of this kind to collect C2 PFCA,[8,15,33,34] while those for longer-chain PFCAs[10,23] are more limited.

Gas-particle partitioning for hydrophobic persistent pollutants (e.g., polybrominated diphenyl ethers[35]) can be effectively described as a function of their octanol-air partitioning coefficient. This relationship cannot fully explain gas-particle partitioning for PFCAs.[10] Although neutral forms of PFCAs have a strong tendency to partition into organic solvent systems,[36–38] those compounds that are expected to be ionized at most environmental pHs, including PFCAs,[39] must also consider the aqueous properties of aerosols, including liquid water content and pH.[10,14] Three modelling studies have attempted to capture the gas-particle partitioning of PFCAs considering the organic and aqueous phases present in the atmospheric condensed phase.[20,22,40] All three were limited in one or more of: the number of homologues considered, the accuracy of the representation of atmospheric particles and/or the range of atmospheric conditions considered. Here we expand upon these studies by describing a three-phase gas-particle partitioning model for C2 – C16 PFCAs under the full range of conditions expected in the atmosphere.

Physical properties (e.g., air-water partitioning coefficient) for PFCAs have been primarily determined by models (e.g., [36]) and limited laboratory studies (e.g., [37]). Although properties for individual homologues often have orders-of-magnitude variations between studies/approaches, trends as a function of PFCA chain length are typically conserved.[41,42] For example, partitioning between water and organic phase increases with increasing PFCA chain length. Measurements of the octanol-water partitioning coefficient (K_{ow}) show a 6 order-of-magnitude larger K_{ow} for the C14 PFCA compared to the C4 PFCA.[37] This suggests that organic matter dominates as a sink for some PFCAs despite their high solubility and ionization tendency in liquid water. Therefore, it is reasonable to speculate that the atmospheric partitioning behavior of short-chain PFCAs will be closer to those of strong inorganic acids, such as HCl and HNO_3, that are mainly controlled by their water solubility and ionization.[43] Long-chain PFCAs are more likely to behave like persistent organic pollutants governed by organic matter mass loadings in ambient PM. Therefore, we propose that by examining gas-partitioning properties of PFCAs with a range

of carbon chain lengths in a gas-aqueous-organic system across the full range of expected atmospheric conditions, we can obtain insight into the atmospheric behaviour and fundamental processes influencing partitioning for different PFCAs.

In this study, we describe the phase partitioning of several PFCAs from C2 to C16 under a range of atmospheric conditions. Our model uses input parameters predicted by multiple thermodynamic models (ppLFER,[44] SPARC,[45] and COSMOtherm[46]) to provide constraints on partitioning. The influence of atmospherically relevant mass loadings of liquid water and organic matter, as the well as the role of surface partitioning, for different PFCAs is analyzed in detail. Modeled possible ranges of the fraction of PFCAs found in particles are compared with published atmospheric measurements that are most likely to be free of artifacts. Implications for our fundamental understanding of PFCA gas-particle partitioning are discussed.

2. Methods and data source

2.1 Model framework of PFCAs gas-particle phase partitioning

The gas-particle partitioning thermodynamic model for PFCAs includes the modeling of gas-aqueous partitioning of PFCAs governed by the air-water partitioning coefficient (K_{AW}). The equilibrium between the neutral PFCAs and deprotonated PFCA(-)s determined by the aqueous phase pH and pK_a values. Last, the partitioning of aqueous phase neutral PFCAs between the aqueous phase and a water-insoluble organic phase in particulate matter (PM) is described by K_{OW} (here we use octanol as a proxy for the water-insoluble organic matter phase). Note that we do not consider the partitioning of anionic PFCAs to the organic matter phase. In detail, we have the equilibria:

$$PFCA_{(aq)} \rightleftharpoons PFCA_{(g)} \qquad K_{AW} = [PFCA_{(g)}]/[PFCA_{(aq)}]$$

$$PFCA_{(aq)} \rightleftharpoons PFCA(-)_{(aq)} + H^{+}_{(aq)}$$

$$K_a = [PFCA(-)_{(aq)}][H^{+}_{(aq)}]/[PFCA_{(aq)}] \quad \text{or} \quad [PFCA(-)_{(aq)}] = [PFCA_{(aq)}] \cdot 10^{pH-pKa}$$

$$PFCA_{(aq)} \rightleftharpoons PFCA_{(om)} \qquad K_{OW} = [PFCA_{(om)}]/[PFCA_{(aq)}]$$

$$PFCA_{(g)} \rightleftharpoons PFCA_{(om)} \qquad K_{OA} = [PFCA_{(om)}]/[PFCA_{(g)}]$$

The equilibrium total particulate phase loading of PFCAs is therefore defined as the summation of all forms of PFCAs in both aqueous phase and organic matter phase:

$$[PFCA_{(p)}] \cdot V_p = [PFCA_{(aq)}] \cdot (V_{H2O} \cdot (1+10^{pH-pKa}) + K_{OW} \cdot V_{OM})$$

$$[PFCA_{(p)}] \cdot V_p = [PFCA_{(aq)}] \cdot V_{H2O} \cdot (1+10^{pH-pKa}) + [PFCA_{(aq)}] \cdot K_{OW} \cdot V_{OM}$$

Where V_p, V_{H2O}, V_{OM} are the volumes for particulate matter, atmospheric water, and particulate organic matter, respectively. Because $[PFCA(-)_{(aq)}] >> [PFCA_{(aq)}]$ under the conditions relevant to this study, this can be simplified as $[PFCA_{(aq)}]+[PFCA(-)_{(aq)}] \approx [PFCA(-)_{(aq)}]$. A concentration-independent expression for the particle phase fraction (ratio of particle phase loading to the total ambient loading) of total ambient PFCA ($\Phi(PFCA)$) can be derived as:

$$\Phi(PFCA) = \frac{[PFCA(p)] \cdot V_p}{[PFCA(p)] \cdot V_p + [PFCA(g)] \cdot V_g}$$

$$\Phi(PFCA) = \frac{V_p/V_g}{\frac{V_p}{V_g} + \frac{K_{AW}}{\frac{V_{H2O}}{V_p}(1 + 10^{pH-pK}) + \frac{V_{OM}}{V_p} \cdot K_{OW}}}$$

where V_p/V_g is the ambient particle volume concentration. The V_{H2O}/V_p and V_{OM}/V_p are the volume fractions of liquid water and organic matter in the particle phase, respectively. The phase partitioning thermodynamic parameters, including K_{AW}, K_{OM}, and pK_a of the target compounds can be obtained from

the literature; databases such as EPA,[47] NCBI;[48] or thermodynamic models.[44] Three extensively used thermodynamic models were used in this study. The pH of particulate liquid water was either quoted from the typical values of particles associated with specific sources (e.g., dust or sea salt) [19] or calculated with the Extended Aerosol Inorganic Model (E-AIM)[49,50] with the input of meteorological parameters and chemical compositions reported alongside PFCA measurements or obtained from other studies reporting those parameters in nearby locations under the same seasonal conditions (i.e. if the chemical composition information is not provided alongside the PFCA measurements).[51] The model framework examines 13 PFCAs (C2: trifluoroacetic acid (TFA), C3: perfluoropropionic acid (PFPrA), C4: perfluorobutanoic acid (PFBA), C5: perfluoropentanoic acid (PFPeA), C6: perfluorohexanoic acid (PFHxA), C7: perfluoroheptanoic acid (PFHpA), C8: perfluorooctanoic acid (PFOA), C9: perfluorononanoic acid (PFNA), C10: perfluorodecanoic acid (PFDA), C11: perfluoroundecanoic aicd (PFUnA), C12: perfluorododecanoic acid (PFDoA), C14: perfluorotetradecanoic acid (PFTeDA), C16: perfluorohexadecanoic acid (PFHxDA)).*2.2 Thermodynamic models used for predicting phase partitioning parameters*

Partitioning properties for PFCAs were predicted using three approaches: 1) poly-parameter linear free energy relationships (ppLFER);[44] 2) SPARC Performs Automated Reasoning in Chemistry (SPARC);[45] and 3) Conductor-like Screening Model for Real Solvents (COSMO-RS or COSMOtherm).[46] The logarithm of the phase partitioning coefficients (logK) predicted by the ppLFER model is based on a linear combination of several predicted parameters describing the properties of the organic solute: relative polarizability (E), dipolarity/polarizability (S), hydrogen bond donor properties (A), hydrogen bond acceptor properties (B), molar volume (V), hexadecane-air partitioning coefficient (L). The ppLFER also predicts solvation properties of phase partitioning systems using: Debye and London forces (e), dipole-

dipole interactions (s), hydrogen bond acceptor properties (a), hydrogen bond donator properties (b), molar volume (v), solvent cavity (l), dispersion interaction energy (c):[52,53]

$$\log K = e \times E + s \times S + a \times A + b \times B + v \times V + l \times L + c$$

The logK values of water/air phase partitioning, octanol/water partitioning, aerosol/air partitioning, water surface/air partitioning at 25 °C, ΔH for the corresponding temperature dependence, and salting constant (K_S: the empirical Setschenow coefficient $[M]^{-1}$, which can be described as: $\log(K_{1/\text{salt water}} / K_{1/\text{water}}) = K_S \cdot [\text{salt}]$) effect on the neutral C2-C8 PFCAs were calculated.[44] Values for pK_a cannot be obtained through ppLFER calculations so the parameters predicted by SPARC were used when needed in this calculation. The commercial online calculator SPARC (https://archemcalc.com/sparc/) was used to predict phase partitioning coefficients depending on the provided molecular structures and phases in the system.[45] In this work, K_{AW}, K_{OW} and pK_a values at 25 °C were predicted with this tool. A quantum chemistry-based software model, COSMO-RS/COSMOtherm [46] is similar to SPARC. Again, K_{AW}, K_{OW} and pK_a values at 25 °C were predicted by COSMOtherm 2020 (BIOVIA-Dassault Systèmes®) on TZVPD-FINE mode.

3. Results and discussion

3.1 PFCA phase partitioning properties

The modeled phase partitioning parameters by the three models are listed in Table S1 along with data from other databases and the literature. As expected, the three models differed in their predicted values, but predicted the same trends, with $\log K_{OW}$ and $\log K_{OA}$ values increasing with PFCA carbon chain length, indicating a higher tendency to partition into the organic phase for longer-chain PFCAs. The difference between the measured and modelled $\log K_{OW}$ values generally spans two units and the pK_a values are within one unit. To test if octanol was an appropriate proxy to represent the partitioning between particulate organic and liquid phases (denoted by $K_{OM/W}$), other partition coefficient values calculated

using several other organic solvent proxies were compared with $\log K_{OW}$ (Figure S1). For ppLFER, dry-octanol, wet-octanol, and ambient aerosols collected onto filters (as described in Arp et al.[54]) were chosen to represent the organic phase in particles. The difference between $K_{OM/W}$ predicted using dry-octanol and wet-octanol was small, but both were about one log unit higher than $K_{OM/W}$ predicted using sampled aerosol. While SPARC modeled $\log K_{OW}$ values were around one log unit higher than ppLFER results, they were close to COSMOtherm predicted $\log K_{OW}$ for C3-C7 PFCAs. In SPARC, the hypothetical structure termB (a hypothetical polycyclic organic molecule with formula $C_{15}H_{18}O_5$, structure shown in Figure S2)[55] was used as an alternative way to represent water-insoluble organic matter as a phase in PM, and similar values to $\log K_{OW}$ were determined. In summary, among all different models/proxies, the differences were generally within three log units. All followed the trend of approximately 0.8 increase in $\log K_{OW}$ for each additional carbon atom in the PFCA.

The temperature dependence and salt effect of the neutral forms of PFCAs on the dry octanol-water partitioning coefficient ($K_{OW(dry)}$) and K_{AW} were tested using the ΔH of phase transfer and the K_S values of salt (NaCl or $(NH_4)_2SO_4$) solution calculated by ppLFER, respectively. The temperature results suggested that the temperature dependent change in $K_{OW(dry)}$ is not significant (< 0.2 log unit, Figure S3) within the relevant ambient temperature range explored (5-35 °C). The $\log K_{AW}$ values of the neutral forms of PFCAs had a stronger response to temperature changes but were generally within one log unit. In contrast, predicted salt effects were found to increase both $K_{OW(dry)}$ and K_{AW} of neutral PFCAs by up to 3.5 log units. At equivalent concentrations of 5 M, $(NH_4)_2SO_4$ solution had stronger salting out effect on a chosen PFCAs compared to NaCl solution. This could be important for urban aerosol where ammonium salts act as the dominant driver of aerosol liquid water content.[56]

3.2 Impact of liquid water content on gas-particle partitioning

Atmospheric liquid water content varies over seven orders of magnitude, which encompasses typical aerosol and fog conditions.[57,58] The acidity of atmospheric aqueous systems exhibits high spatial and temporal heterogeneity, which can range from pH values of -1 to 5 for aerosol liquid water and 2 to 7 for fog droplets.[19] The phase partitioning of C2-C8 PFCAs was modeled over the full range of liquid water conditions under two pH scenarios: pH-pK_a = 3 and pH-pK_a = 6 to represent strongly and weakly acidic conditions, respectively (Figure 1). The pK_a values for the chosen PFCAs are generally within the range of -0.2 to 1.0 (Table S1),[36,59] so these two scenarios correspond to a pH of atmospheric liquid water ranging from 2.8-4 and 5.8-7, respectively. A constant difference between pH and pK_a was chosen instead of the absolute pH values to avoid uncertainties in pK_a values modeled or measured by different approaches. The organic matter ambient concentration was fixed at 10 μg m^{-3} for both scenarios. The effect of organic matter concentrations on PFCA particle fractions, as well as potential impacts from their surfactant properties, will be discussed in the sections that follow. Figure 1 represents the upper bound of these compounds in the particle phase fraction for two reasons. Firstly, $(NH_4)_2SO_4$ and NaCl, which are found in real aerosols and were not considered in our model, have been predicted to have a salting out effect on PFCAs (shown in Figure S3).[44] Secondly, although we assumed partitioning into organic matter followed K_{OW}, PFCA partitioning into organic matter proxies other than octanol are predicted to be less favorable.[44]

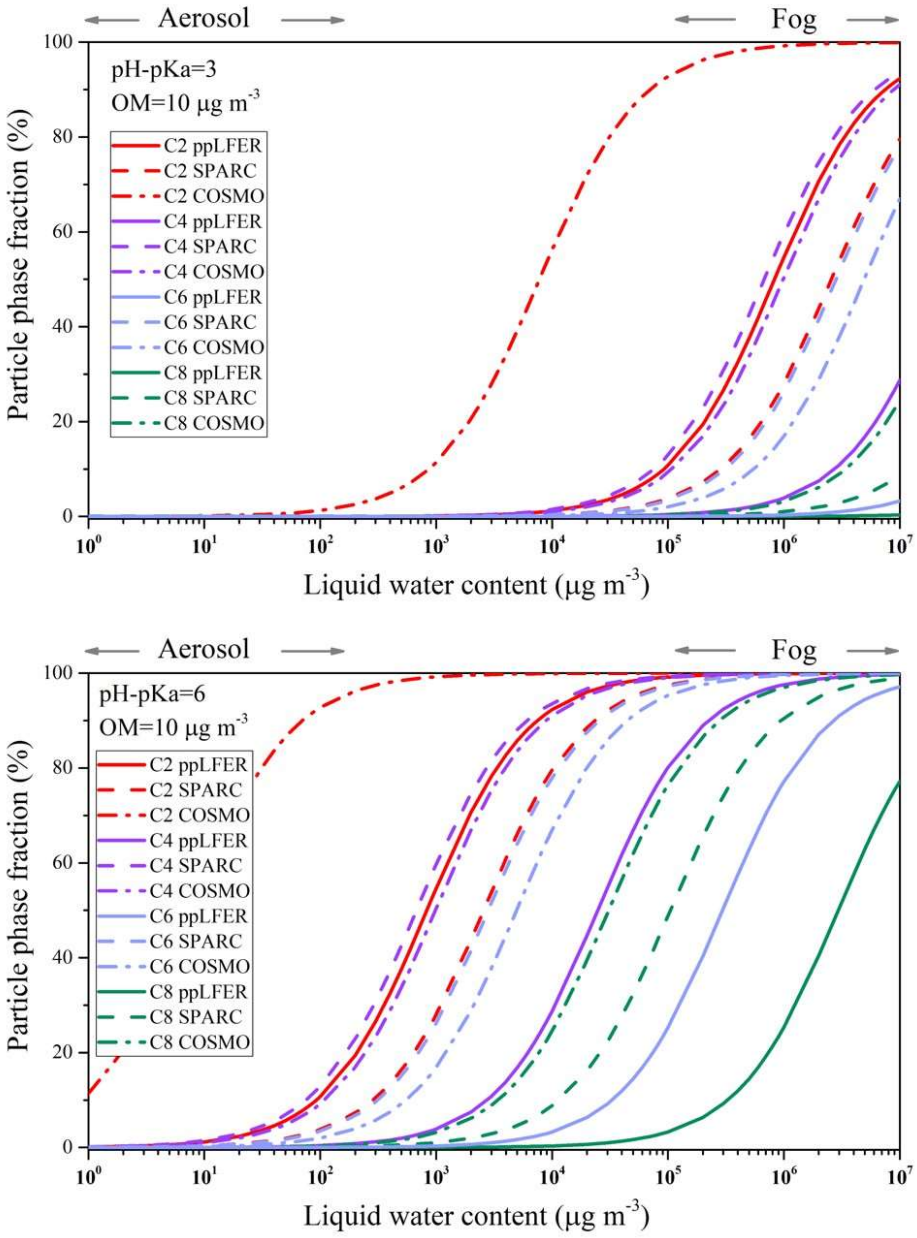

Figure 1. Modeled particle phase fraction of selected PFCAs (C2: TFA, C4: PFBA, C6: PFHxA, and C8: PFOA) with thermodynamic parameters calculated by three thermodynamic models (ppLFER, SPARC, COSMOtherm) under set scenarios with organic matter mass loading constant at 10 μg m^{-3} (upper panel: strongly acidic aerosol pH-pK_a=3, lower panel: close to neutral aerosol pH-pK_a=6).

Our model results indicated that shorter-chain PFCAs are more likely to partition into aerosol liquid water, while longer-chain PFCAs have a higher tendency to remain in the gas phase. Though predictions showed expected variability based on the differences from the three models used (i.e. logK values spanning two units), predicted trends for PFCAs of different chain lengths were generally consistent for all models. The pH of the water body can significantly change the gas-particle phase partitioning behavior, with a much greater fraction of PFCAs partitioning into water in the weakly acidic case (pH-pK_a = 6). In the more acidic condition (pH-pK_a = 3) for the case of liquid water content corresponding to those typical of aerosols, all PFCAs were predicted to be >99 % in the gas phase. This prediction was independent of the physical properties used. In the more acidic condition with high liquid water content corresponding to fog droplets, the predicted phase partitioning behavior depended on the PFCA properties predicted by the different models. The largest discrepancy was observed for TFA phase partitioning in fog conditions (typical liquid water content = 10^6 μg m^{-3} [60]). The impact of the different modeled physical properties on phase partitioning was apparent for all PFCAs in the weakly acidic condition (pH-pK_a = 6). The gas-particle phase partitioning of each PFCA will be sensitive to their model-predicted physical properties under different conditions. Shorter-chain PFCAs have a higher tendency to partition to the condensed phase, so as a result their gas fraction is more sensitive under lower liquid water content conditions. Under the more acidic conditions (pH-pK_a = 3), TFA, the shortest-chain PFCA, is sensitive to predicted physical properties under atmospherically relevant liquid water content. This outcome means that compared with the other PFCAs, the uncertainties in the modeled physical properties of TFA are more likely to propagate into increased uncertainty in its phase partitioning behavior. In contrast, predicted physical properties only affect the phase partitioning of C4-C6 PFCAs in the liquid water regime corresponding to fog conditions, while the phase partitioning of the C8 PFCA depends little on modeled physical properties across all atmospherically relevant liquid water contents. Lastly, in the weakly acidic scenario (pH-pK_a = 6), there

is a liquid water content range over which each PFCA is sensitive to the physical properties predicted by the different models in use by the environmental chemistry community. Overall, the sensitive region that impacts gas-particle partitioning of shorter-chain PFCAs corresponds to aerosol liquid water content conditions, and the region that impacts longer-chain PFCAs corresponds to fog liquid water content conditions.

3.3 Impact of organic matter content on gas-particle partitioning

To encompass the extremes of organic matter concentrations found in the atmosphere, the impact of a range of organic matter concentrations spanning 10^{-1} to 10^{3} μg m^{-3} on PFCA gas-particle partitioning was tested. These organic matter concentration ranges were examined under four scenarios (Figure 2): (a) a liquid water concentration representative of aerosol (10 μg m^{-3}) and strongly acidic (pH-pK_a = 3); (b) a liquid water concentration representative of fog (10^{6} μg m^{-3}) and strongly acidic (pH-pK_a = 3); followed by the same two water conditions, but under weakly acidic (pH-pK_a=6) conditions (Figure 2 c-d). In the fog water cases (Figure 2b, d), organic matter content had a negligible impact on C2-C8 PFCA gas-particle partitioning, while it did influence the gas-particle partitioning of C10-C16 PFCAs (Figure S4b, d). Across these aerosol liquid water content scenarios, partitioning to the gas phase was strongly favoured for C2-C16 PFCAs (Figure 2a, c, Figure S4a ,c). They were predicted to be more than 95 % in the gas phase when organic matter mass loadings were <100 μg m^{-3}, except for the case using COSMOtherm-predicted properties for TFA. This suite of scenarios encompasses most atmospheric conditions, with the exception of extreme pollution events. Under all conditions of aerosol liquid water content, organic matter concentrations did not affect the gas-particle partitioning of C2 and C4 but could alter those of PFCAs with 6 or more carbons under high particulate organic matter loading

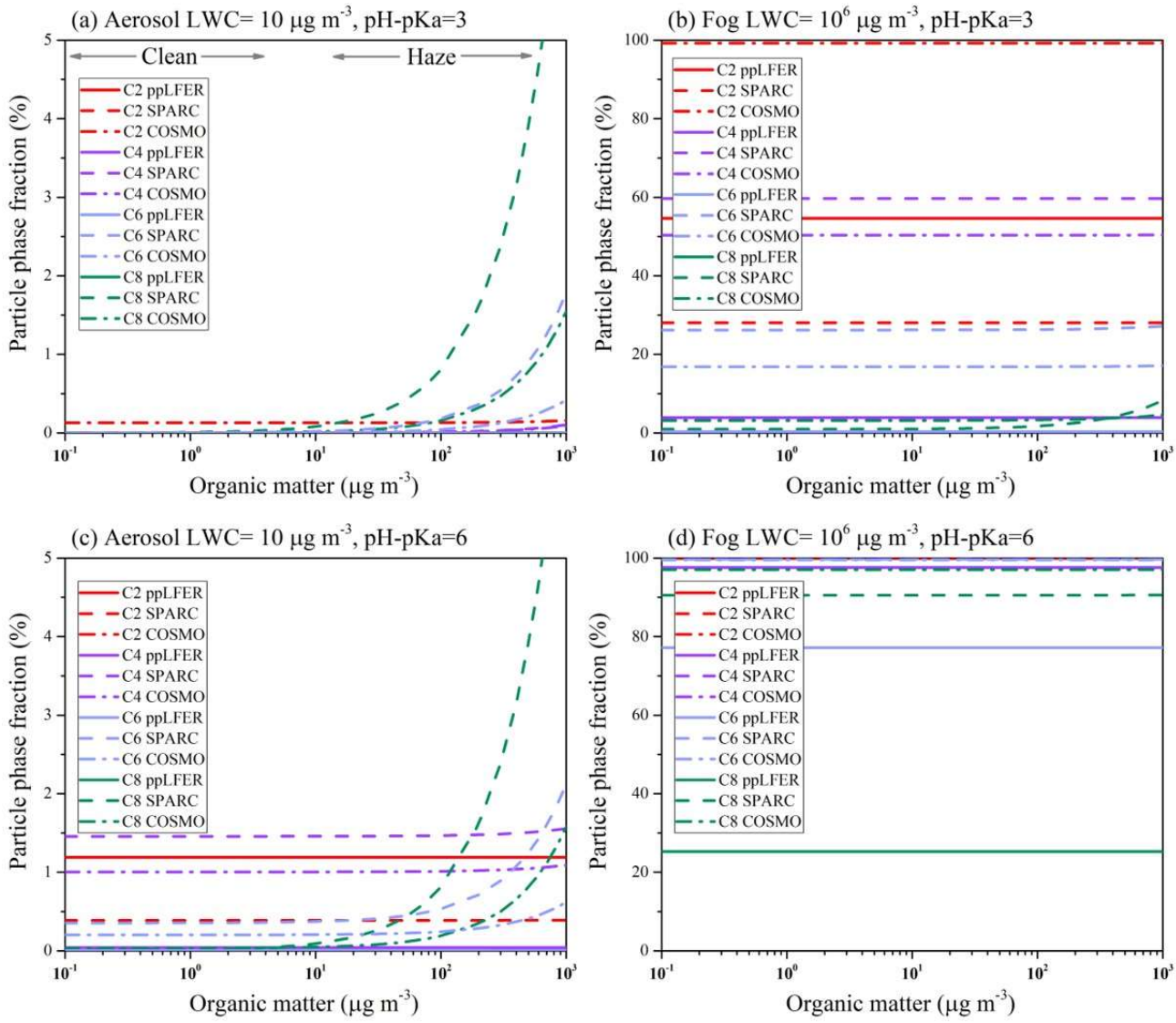

Figure 2. Modeled particle phase fraction of selected PFCAs (C2: TFA, C4: PFBA, C6: PFHxA, and C8: PFOA) with thermodynamic parameters calculated by three thermodynamic models (ppLFER, SPARC, COSMOtherm) under set scenarios (a)strongly acidic aerosol, (b) strongly acidic fog, (c) weakly acidic aerosol, and (d) weakly acidic fog. Note the different scales on the y axis between the aerosol (left) and fog (right) panels. Values for C2 COSMOtherm-predicted are offscale in (c) and reach 56 % at 10^3 μg m^{-3}.

conditions (Figure 2a, c and Figure S4a, c). This pattern can be explained by the fact that as carbon chain length increases, the PFCAs have a stronger tendency to partition into the organic phase. Therefore, when K_{OW} becomes large enough or there is a substantial amount of organic matter in the particle phase, the

interactions between the PFCA and organic matter can dominate over the PFCA interactions with water. This can be expressed quantitatively as the ratio of the ambient concentrations of PFCAs partitioned in particulate water-insoluble organic matter to that in aqueous phase:

$$\frac{[\mathrm{PFCA(om)}] \cdot \mathrm{V_{OM}}}{[\mathrm{PFCA(^-)(aq)}] \cdot \mathrm{V_{H2O}}} = 10^{\mathrm{LogKow-(pH-pKa)}} \cdot \frac{\mathrm{V_{OM}}}{\mathrm{V_{H2O}}}$$

From this equation, it is clear that organic matter becomes the dominant sink for PFCAs under two conditions: first, when $\log K_{OW}$ is larger than pH-pK_a (with value equal to 3 or 6 explored in this framework) and/or second, when organic matter volume is equal to or greater than that of water. Under the aerosol-representing lower liquid water content case, these conditions are met for longer-chain PFCAs (C10-C16, Table S1) when organic matter levels are also high. Unless in severe organic matter pollution episodes, organic matter content will not affect the C2-C8 PFCAs, which were predicted to mainly partition between the air and aqueous phase like strong inorganic acids (e.g., HCl, HNO_3). As a result, their gas-particle partitioning is independent of organic matter concentration and is driven primarily by the factors described in Section 3.1. For PFCAs with carbon chains longer than 12, their $\log K_{OW}$ values were predicted to be larger than 8 by both ppLFER and SPARC. As a result, $\log K_{OW} > (\mathrm{pH} - pK_a)$, which causes organic matter to become a more dominant particle phase sink for these longer chain PFCAs (Figure S4) and their behaviour can be thought of as similar to neutral organic pollutants. Based on the liquid water and organic matter dependencies explored, the threshold between PFCAs behaving like inorganic atmospheric acids and neutral organic pollutants lies between C8 and C12. Therefore, a better understanding of K_{AW} should be prioritized to reliably model the atmospheric phase partitioning of short-chain PFCAs, while improved understanding of K_{OW} is crucial to constrain the phase partitioning behavior of long chain PFCAs.

3.4 Impact of PFCA surfactant properties on gas-particle partitioning

Our modelling framework has not considered the potential enhanced accumulation of PFCAs at surfaces. We explored this limitation using K_i values (air-water interfacial adsorption coefficients) at 0.1 mg L^{-1} derived from measurements of sodium salts of PFCAs in a deionized water system.[61] These values were scaled to approximate the resulting bulk-to-surface ratio of PFCAs in spherical aqueous aerosols with diameters from 0.05 to 2.5 μm by considering their surface area-to-volume ratios (Figure 3a). Although we consider this large aerosol size range, it should be noted that the average diameter of ambient aerosol is generally larger than 0.1 μm.[62–66] We also note that concentration,[67] the counter-cation,[68,69] and ionic strength[69] are all known to affect K_i, so the results presented here are a simplification based on limited relevant data. As expected for these well-known surfactants, accumulation of ionized PFCAs at the interface increased with increasing chain length and decreasing particle diameter. For C2-C3 PFCAs, there was no accumulation at surfaces regardless of particle size. For C4-C6 PFCAs, accumulation was dependent on particle diameter. For PFCAs ≥C7, there was always enhancement at the surface interface. Thus, we expect that our predictions for gas-particle partitioning in aqueous particles will be more accurate for shorter-chain PFCAs. However, with increasing PFCA chain length, we expect increased partitioning into organic matter, as discussed above. To explore the importance of surface enhancement for neutral PFCAs in organic matter, the surface partitioning coefficients (K_{SURF}, defined as the equilibrium concentration ratio of PFCAs in the unit area of surface to that in the unit volume of air bulk) of C2-C8 PFCAs were also predicted by ppLFER.[44] With these prediction results alongside the bulk phase partitioning coefficients predicted by ppLFER, the relative importance of bulk phase partitioning and surface partitioning between the gas and aerosol phases could be quantified. We considered an extreme case with small spherical pure organic matter particles (0.1 μm diameter), that would have amongst the largest surface area-to-volume ratio, at a loading of 10 μg m^{-3}. Partitioning to the bulk dominated, though there was a strong dependence on PFCA chain length (Figure 3b). The C2 PFCA was predicted to have

more than 50 times in the bulk than the surface. This increased to a bulk enhancement of greater than 10^9 for the C8 PFCA. Thus, for all PFCAs in organic matter, the bulk is predicted to be the dominant particle reservoir. Given the complexities in phase separation and resulting particle morphologies that are the subject of ongoing research (e.g. [17,18]), further work will be needed to understand this fully.[62–66]

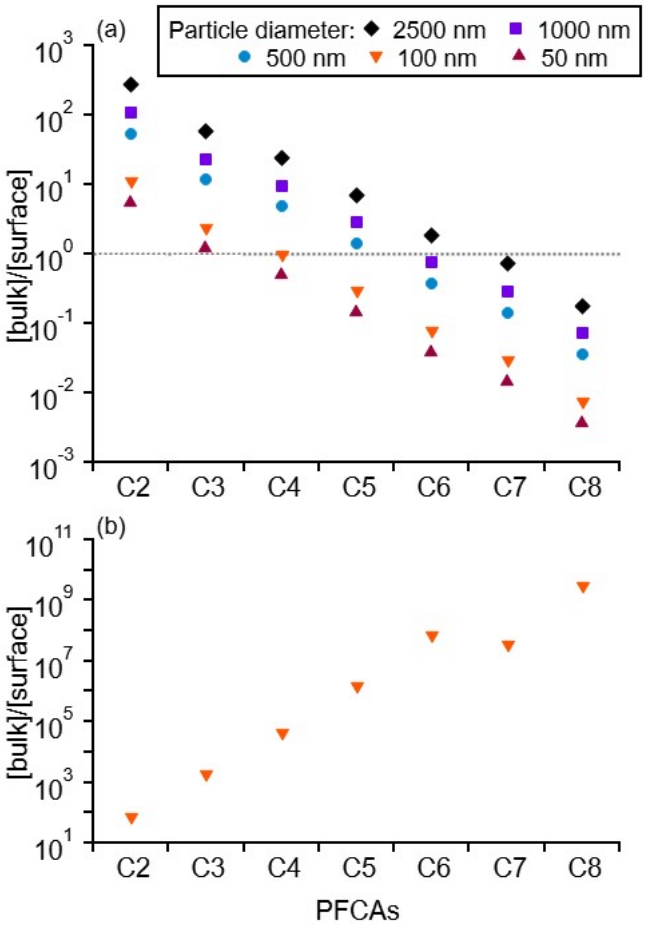

Figure 3. Surface enhancement for PFCAs in spherical particles for a) aqueous particles of different diameters determined from K_i (data from [61]) and b) 0.1 µm diameter organic matter particles calculated by ppLFERs.[44]

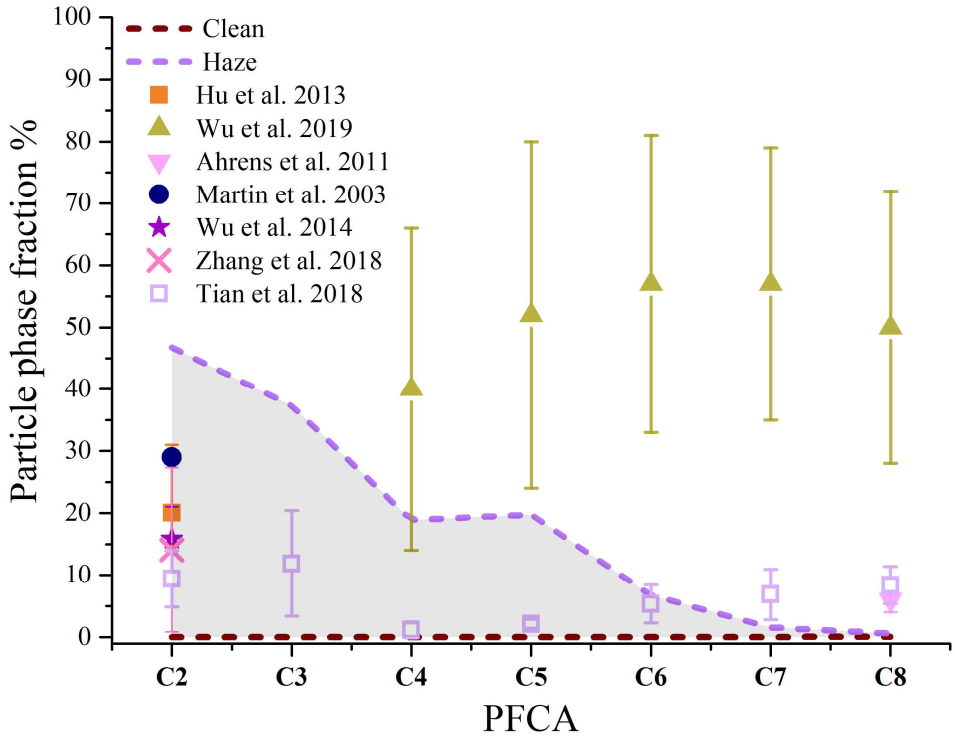

Figure 4. Comparison between modeled ranges of possible particle phase fraction of C2-C8 PFCAs and several observational results. [8,10,15,23,29,33,34,70]

3.5 Comparison to PFCA gas and particle observations

A further evaluation of our modeled partitioning was performed by comparing to several literature observations of PFCAs as gases and in particles. Seven studies were selected that used sampling techniques that minimize sampling bias (details in Table S2).[10,26] Six of these studies used annular denuder followed by filter pack sampling apparatus, outfitted with selection for particles with aerodynamic diameter less than 2.5 μm[10,15,23,29,33,34] or 10 μm,[8] while one other study used a passive sampler for gas phase and dry deposition sampler to sample particle deposition, which they used as a proxy for total suspended particles.[70] To facilitate comparison, the particle phase fraction ranges of PFCAs from C2 to C8 were predicted under two scenarios: one characterized by atmospheric composition under relatively

clean conditions and a second that represents a highly polluted atmosphere. These clean and haze scenarios define the lower bound and upper bound of the particle fraction range, respectively. The haze scenario was defined with a much higher ambient mass loading of aerosol liquid water, organic matter concentration, and elevated pH value,[36,59] which all favoured PFCA accumulation into the particle phase. Calculations were based on the following parameters: pH, inorganic chemical composition (used to determine liquid water content), organic matter fraction (used to determine organic matter concentration), and particle loadings (Table S1). The minimum and maximum particle phase values obtained across the clean and haze scenarios were then compared with the observations from the seven studies (Figure 4). For most of the investigated studies, there was a general trend of decreasing agreement between the range of model predictions and the measurements with increasing chain length, where longer-chain PFCAs were measured in particles at higher levels than predicted by our model. The exception is the study of Wu et al.,[23] in which measurements of C4 to C8 PFCAs in particles were always much higher than predicted. For C2 and C3 PFCAs, all measured particle phase fractions[8,33,34,70] fell within the predicted possible range. For C4 to C6 PFCAs, the particle fraction measurements by Wu et al.[23] were higher than the maximum modeled value by 2 to 9 times, while those from Tian et al.[70] agreed with the model. For C7 and C8 PFCAs, all three studies[10,23,29,70] measured particle phase fractions higher than those predicted by the model. Those of Tian et al.[70] and Ahrens et al.[10,29] were 4 to 14 times higher than the upper limit from the modeled haze scenario, while measurements of Wu et al.[23] were nearly two orders of magnitude higher than the upper limit from the model. It is worthwhile to note that several other observations of PFCA gas-particle partitioning that did not use denuders to remove gas phase PFCAs prior to particle sampling observed particle fractions 20 to 70 % higher than the predicted upper bound (shown in Figure S5).[29,71–73] It is unclear why such a large discrepancy between modeled and the measured particle fractions from Wu et

al.[23] exists. To explore model-measurement discrepancies further, atmospheric conditions specific to each of the PFCA measurements were considered.

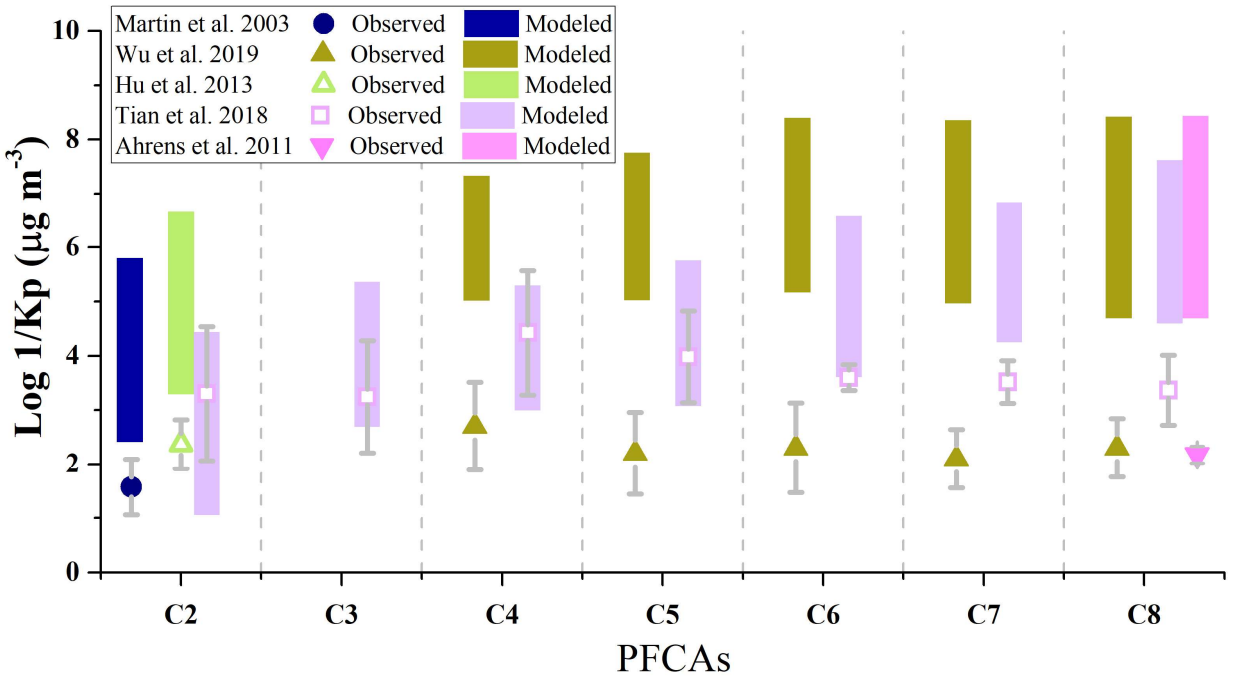

Figure 5. Comparison between the modeled possible ranges of Log 1/K_P values of C2-C8 PFCAs and selected observational results[8,10,23,29,34,70] using location-specific parameters showing that the model generally underpredicts observed particle fractions.

The gas-particle partitioning equilibria for five of the studies shown in Figure 4 were examined in greater detail. Instead of using general scenarios, the observed mean and the possible modeled ranges of log1/K_P (K_P is particle-gas partitioning ratio) values were calculated for each study using information specific to their respective observation periods. The K_P values were defined using a ratio where the mass fraction (ng of PFCA in the PM per µg of total PM) was found relative to the mass concentration in the ambient gas phase (ng PFCA per m^3 of air). The modeled K_P ranges were then based on the specified sampled PM mass loadings and the typical chemical composition reported at the sampling site alongside

the PFCA results or obtained from other studies conducted in the same region (details in Section 1 of supplementary information[40,74–79]). The pH values of the aerosol liquid water are modelled from 3 to 6.5 with the aerosol in Canadian monitoring sites being more acidic than those in Beijing. Both values and trends of pH values used in this study are supported by aerosol acidity studies conducted in the same regions.[74,80,81] Though the pH values could be impacted by some short period intense events (e.g., dust events, pollutant plumes, etc.), the average values of aerosol pH through the month-long sampling period should be well represented. The modeled ranges were obtained using the thermodynamic equilibrium constants listed in Table S1. Generally, the model predicted higher $\log 1/K_p$ values than were reported in the measurements (Figure 5). This means the K_p was underpredicted by the model and that there is greater particulate accumulation of PFCAs than can be explained by our considered chemical and physical equilibrium thermodynamic properties alone. This trend becomes more pronounced for the longer-chain PFCAs. Disagreements between model and measurement range from less than one log unit for C2 PFCA[8,34,70] to 1-2.5 log units for C8 PFCA.[10,23,29,70] For the measurements of Tian et al.,[70] the measurement and model particle fractions agree for shorter-chain PFCAs, but the model underpredicts particle fractions for C7 and C8 PFCAs. The disagreement between model and measurements by Wu et al.[23] was independent of chain length, with the model under-predicting the particle fraction consistently by more than two orders of magnitude for C4-C8 PFCAs. Even though uncertainties in the meteorological parameters and chemical composition estimation could contribute to some disagreement, these uncertainties are unlikely to cause the magnitude of the differences found in this comparison (e.g. see impact of changing OM loading in Section 3.3).

3.6 Implications for understanding PFCA gas-particle partitioning

Our overall findings demonstrate that from a theoretical perspective, PFCAs will largely reside in the gas phase with limited partitioning to particles. The hypothesis that short-chain PFCAs partition similarly

to strong inorganic acids and that long-chain PFCAs partition similarly to neutral pollutants is supported by this work. Gas-particle partitioning of short-chain PFCAs is dominated by partitioning to the aqueous fraction of particles. Their degree of partitioning to particles is sensitive liquid water content and to their physical properties. An improved knowledge of K_{AW} for these PFCAs would improve our understanding of their atmospheric partitioning. Long-chain PFCAs have a greater sensitivity to the presence and quantity of organic matter. Uncertainties in the gas-particle partitioning of long-chain PFCAs includes their known surfactant properties and salting out effects. Predictions of gas-particle partitioning of long-chain PFCAs would improve as a result of better understanding of the physical properties that drive their partitioning to organics and interfaces. Comparisons to ambient measurements highlight the utility of this framework for understanding the gas-particle partitioning of PFCAs and demonstrate that there are additional considerations that may be missing from the framework.

It is notable that our model underestimated the PFCA particle fraction for all four studies that used annular denuder-filter pack sampling apparatus (Figure 5). This did not depend on whether the collected particles had diameters less than 2.5 μm[10,23,34] or 10 μm,[8] as disagreement with this thermodynamic model framework remained. This suggests the existence of missing partitioning and/or other mechanisms driving the accumulation of particulate PFCAs, which we will explore further here. One potential explanation is that a specific particle type plays an important role in driving partitioning, and those particles are not internally mixed. For example, hygroscopic dust particles, either in coarse mode (>2.5 μm) or externally mixed in the fine mode (<2.5 μm), could be an important sink for particulate PFCAs due to their hygroscopic and/or alkaline characteristics. Such chemistry has been observed for several low-molecular-weight organic acids and strong inorganic acids.[82–85] This is consistent with observations of relatively high levels of PFCAs in dust and coarse mode aerosol[86,87] and is implied within observations that PFCA deposition correlated moderately with that of dust components (i.e., non-sea salt Ca^{2+} and Mg^{2+}) in Arctic

ice core samples.[88] The assumption of internal mixing in models, which does not represent dust as a separate particle population, is likely to lead to underestimation of the deprotonated fraction of the PFCAs, leading to lower predicted particle fractions. In addition, if this process is an important sink for PFCAs, the model agreement with the Tian et al.[70] total suspended particle measurement is coincidental, because thermodynamic equilibrium partitioning models cannot capture reactive chemistry happening in the coarse mode.

Several studies examining gas-particle partitioning of atmospheric organic acids have also reported similar model-measurement discrepancies.[32,89–94] Proposed explanations include the strong effect of activity coefficients and the formation of complexes or organic salts. Both could contribute to the discrepancies observed here for PFCAs. Other possible explanations include our assumption in this modeling framework that the deprotonated PFCAs have no interaction with organic matter and our exclusion of surfactant properties. In all, more advanced knowledge of PFCA thermodynamic phase partitioning equilibria, reversible and/or irreversible uptake by ambient particulate matter are required to explain the discrepancy identified in this study. More reliable measurements of ambient PFCAs in both gas and particle phases with high time resolution, as well as uptake experiments on surfaces of different composition, physical state, and morphology conducted in laboratory experiments will be beneficial to generate reliable parameters to underpin environmental fate modeling of ambient PFCAs.

Supplementary information

Includes: comparison of the different Log $K_{organic/water}$ values modeled by different models and proxies (Figure S1), chemical structure of water-insoluble organic matter TermB (Figure S2), the modeled temperature dependence and salt effect of phase partitioning equilibrium constants (Figure S3), modeled particle phase fraction of C10-C16 as a function of organic matter mass loadings (Figure S4), comparison

between the modeled particle phase fraction ranges and several observation results that sampled particles prior to gas phase removal (Figure S5), a summary of the modeling results and literature values for the thermodynamic parameters (Table S1), a summary of the sampling information of the studies used for detailed phase partitioning analysis (Table S2), and a description of the reference chemical composition and acidity of PM from the five representative studies (Section 1).

Acknowledgement

Funding was provided by the Natural Science and Engineering Research Council of Canada and Environment and Climate Change Canada. RY was supported by an Ontario Graduate Scholarship. We thank Sivani Baskaran and Frank Wania for access to COSMOtherm.

References

1 A. B. Lindstrom, M. J. Strynar and E. L. Libelo, Polyfluorinated compounds: Past, present, and future, *Environmental Science and Technology*, 2011, **45**, 7954–7961.

2 J. Glüge, M. Scheringer, I. T. Cousins, J. C. Dewitt, G. Goldenman, D. Herzke, R. Lohmann, C. A. Ng, X. Trier and Z. Wang, An overview of the uses of per- And polyfluoroalkyl substances (PFAS), *Environmental Science: Processes and Impacts*, 2020, **22**, 2345–2373.

3 D. Muir, R. Bossi, P. Carlsson, M. Evans, A. de Silva, C. Halsall, C. Rauert, D. Herzke, H. Hung, R. Letcher, F. Rigét and A. Roos, Levels and trends of poly- and perfluoroalkyl substances in the Arctic environment – An update, *Emerging Contaminants*, 2019, **5**, 240–271.

4 I. T. Cousins, J. C. Dewitt, J. Glüge, G. Goldenman, D. Herzke, R. Lohmann, C. A. Ng, M. Scheringer and Z. Wang, The high persistence of PFAS is sufficient for their management as a chemical class, *Environmental Science: Processes and Impacts*, 2020, **22**, 2307–2312.

5 C. A. Ng and K. Hungerbühler, *Environmental Science and Technology*, 2014, 48, 4637–4648.

6 E. M. Sunderland, X. C. Hu, C. Dassuncao, A. K. Tokranov, C. C. Wagner and J. G. Allen, *Journal of Exposure Science and Environmental Epidemiology*, 2019, 29, 131–147.

7 L. Zhang, H. Sun, Q. Wang, H. Chen, Y. Yao, Z. Zhao and A. C. Alder, Uptake mechanisms of perfluoroalkyl acids with different carbon chain lengths (C2-C8) by wheat (Triticum acstivnm L.), *Science of The Total Environment*, 2019, **654**, 19–27.

8 J. W. Martin, S. a Mabury, C. S. Wong, F. Noventa, K. R. Solomon, M. Alaee and D. C. G. Muir, Airborne haloacetic acids, *Environmental Science & Technology*, 2003, **37**, 2889–2897.

9 L. Ahrens, M. Shoeib, T. Harner, S. C. Lee, R. Guo and E. J. Reiner, Wastewater treatment plant and landfills as sources of polyfluoroalkyl compounds to the atmosphere, *Environmental Science and Technology*, 2011, **45**, 8098–8105.

10 L. Ahrens, T. Harner, M. Shoeib, D. A. Lane and J. G. Murphy, Improved characterization of gas-particle partitioning for per- and polyfluoroalkyl substances in the atmosphere using annular diffusion denuder samplers, *Environmental Science and Technology*, 2012, **46**, 7199–7206.

11 J. H. Johansson, M. E. Salter, J. C. Acosta Navarro, C. Leck, E. D. Nilsson and I. T. Cousins, Global transport of perfluoroalkyl acids via sea spray aerosol, *Environmental Science: Processes and Impacts*, 2019, **21**, 635–649.

12 C. P. Thackray, N. E. Selin and C. J. Young, Global atmospheric chemistry model for the fate and transport of PFCAs and their precursors, *Environmental Science Processes and Impacts*, 2020, **22**, 285–293.

13 C. J. Young and S. A. Mabury, Atmospheric perfluorinated acid precursors: Chemistry, occurrence and impacts, *Reviews of Environmental Contamination and Toxicology*, 2010, **208**, 1–110.

14 E. L. D'Ambro, H. O. T. Pye, J. O. Bash, J. Bowyer, C. Allen, C. Efstathiou, R. C. Gilliam, L. Reynolds, K. Talgo and B. N. Murphy, Characterizing the air emissions, transport, and deposition of per- and polyfluoroalkyl substances from a fluoropolymer manufacturing facility, *Environmental Science and Technology*, 2021, **55**, 862–870.

15 J. Wu, J. W. Martin, Z. Zhai, K. Lu, L. Li, X. Fang, H. Jin, J. Hu and J. Zhang, Airborne trifluoroacetic acid and its fraction from the degradation of HFC-134a in Beijing, China, *Environmental Science and Technology*, 2014, **48**, 3675–3681.

16 J. H. Seinfeld and S. N. Pandis, *Atmospheric Chemistry and Physics*, John Wiley & Sons, Inc., Hoboken, NJ, 2nd Editio., 2006.

17 Y. You, L. Renbaum-Wolff, M. Carreras-Sospedra, S. J. Hanna, N. Hiranuma, S. Kamal, M. L. Smith, X. Zhang, R. J. Weber, J. E. Shilling, D. Dabdub, S. T. Martin and A. K. Bertram, Images reveal that atmospheric particles can undergo liquid–liquid phase separations, *Proceedings of the National Academy of Sciences*, 2012, **109**, 13188–13193.

18 M. Song, P. Liu, S. T. Martin and A. K. Bertram, Liquid–liquid phase separation in particles containing secondary organic material free of inorganic salts, *Atmospheric Chemistry and Physics*, 2017, **17**, 11261–11271.

19 H. P. H. Arp and K. U. Goss, Gas/particle partitioning behavior of perfluorocarboxylic acids with terrestrial aerosols, *Environmental Science and Technology*, 2009, **43**, 8542–8547.

20 L. Vierke, L. Ahrens, M. Shoeib, E. J. Reiner, R. Guo, W. U. Palm, R. Ebinghaus and T. Harner, Air concentrations and particle-gas partitioning of polyfluoroalkyl compounds at a wastewater treatment plant, *Environmental Chemistry*, 2011, **8**, 363–371.

21 S. K. Kim, D. Li and K. Kannan, In situ measurement-based partitioning behavior of perfluoroalkyl acids in the atmosphere, *Environmental Engineering Research*, 2020, **25**, 281–289.

22 J. Wu, H. Jin, L. Li, Z. Zhai, J. W. Martin, J. Hu, L. Peng and P. Wu, Atmospheric perfluoroalkyl acid occurrence and isomer profiles in Beijing, China, *Environmental Pollution*, , DOI:10.1016/j.envpol.2019.113129.

23 W. Liu, W. He, J. Wu, W. Wu and F. Xu, Distribution, partitioning and inhalation exposure of perfluoroalkyl acids (PFAAs) in urban and rural air near Lake Chaohu, China, *Environmental Pollution*, 2018, **243**, 143–151.

24 B. R. Appel, S. M. Wall, Y. Tokiwa and M. Haik, Interference effects in sampling particulate nitrate in ambient air, *Atmospheric Environment*, 1979, **13**, 319–325.

25 United States Environmental Protection Agency, *Compendium of Methods for the Determination of Inorganic Compounds in Ambient Air: Determination of reactive acidic and basic gases and strong acidity of atmospheric fine particles (<2.5 μm) (Compendium Method IO-4.2)*, 1999.

26 W. Nie, T. Wang, X. Gao, R. K. Pathak, X. Wang, R. Gao, Q. Zhang, L. Yang and W. Wang, Comparison among filter-based, impactor-based and continuous techniques for measuring atmospheric fine sulfate and nitrate, *Atmospheric Environment*, 2010, **44**, 4396–4403.

27 J. A. Faust, PFAS on atmospheric aerosol particles: a review, *Environmental Science: Processes & Impacts*, , DOI:10.1039/D2EM00002D.

28 L. Ahrens, M. Shoeib, T. Harner, D. A. Lane, R. Guo and E. J. Reiner, Comparison of annular diffusion denuder and high volume air samplers for measuring per- and polyfluoroalkyl substances in the atmosphere, *Analytical Chemistry*, 2011, **83**, 9622–9628.

29 H. P. H. Arp and K.-U. Goss, Irreversible sorption of trace concentrations of perfluorocarboxylic acids to fiber filters used for air sampling, *Atmospheric Environment*, 2008, **42**, 6869–6892.

30 K. Kristensen, M. Bilde, P. P. Aalto, T. Petäjä and M. Glasius, Denuder/filter sampling of organic acids and organosulfates at urban and boreal forest sites: Gas/particle distribution and possible sampling artifacts, *Atmospheric Environment*, 2016, **130**, 36–53.

31 A. Lutz, C. Mohr, M. le Breton, F. D. Lopez-Hilfiker, M. Priestley, J. A. Thornton and M. Hallquist, Gas to Particle Partitioning of Organic Acids in the Boreal Atmosphere, *ACS Earth and Space Chemistry*, 2019, **3**, 1279–1287.

32 B. Zhang, Z. Zhai and J. Zhang, Distribution of trifluoroacetic acid in gas and particulate phases in Beijing from 2013 to 2016, *Science of the Total Environment*, 2018, **634**, 471–477.

33 X. Hu, J. Wu, Z. H. Zhai, B. Y. Zhang and J. B. Zhang, Determination of gaseous and particulate trifluoroacetic acid in atmosphere environmental samples by gas chromatography-mass spectrometry, *Fenxi Huaxue/ Chinese Journal of Analytical Chemistry*, 2013, **41**, 1140–1145.

34 M. Shoeib, T. Harner, M. Ikonomou and K. Kannan, Indoor and outdoor air concentrations and phase partitioning of perfluoroalkyl sulfonamides and polybrominated diphenyl ethers, *Environmental Science and Technology*, 2004, **38**, 1313–1320.

35 Z. Wang, M. MacLeod, I. T. Cousins, M. Scheringer and K. Hungerbühler, Using COSMOtherm to predict physicochemical properties of poly- and perfluorinated alkyl substances (PFASs), *Environmental Chemistry*, 2011, **8**, 389–398.

36 Q. Xiang, G. Shan, W. Wu, H. Jin and L. Zhu, Measuring log Kow coefficients of neutral species of perfluoroalkyl carboxylic acids using reversed-phase high-performance liquid chromatography, *Environmental Pollution*, 2018, **242**, 1283–1290.

37 J. Hammer, J. J.-H. Haftka, P. Scherpenisse, J. L. M. Hermens and P. W. P. de Voogt, Fragment-based approach to calculate hydrophobicity of anionic and nonionic surfactants derived from chromatographic retention on a C_{18} stationary phase, *Environmental Toxicology and Chemistry*, 2017, **36**, 329–336.

38 L. Vierke, U. Berger and I. T. Cousins, Estimation of the acid dissociation constant of perfluoroalkyl carboxylic acids through an experimental investigation of their water-to-air transport, *Environmental Science and Technology*, 2013, **47**, 11032–11039.

39 B. Zhang, Z. Zhai and J. Zhang, Distribution of trifluoroacetic acid in gas and particulate phases in Beijing from 2013 to 2016, *Science of the Total Environment*, 2018, **634**, 471–477.

40 H. P. H. Arp, C. Niederer and K.-U. Goss, Predicting the partitioning behavior of various highly fluorinated compounds, *Environmental Science and Technology*, 2006, **40**, 7298–7304.

41 S. Rayne and K. Forest, Perfluoroalkyl sulfonic and carboxylic acids: A critical review of physicochemical properties, levels and patterns in waters and wastewaters, and treatment methods, *Journal of Environmental Science and Health, Part A*, 2009, **44**, 1145–1199.

42 Y. Tao, A. Moravek, T. C. Furlani, C. E. Power, T. C. VandenBoer, R. Y.-W. Chang, A. Wiacek and C. J. Young, Acidity of Size-Resolved Sea-Salt Aerosol in a Coastal Urban Area: Comparison of Existing and New Approaches, *ACS Earth and Space Chemistry*, 2022, **6**, 1239–1249.

43 N. Ulrich, S. Endo, T. N. Brown, N. Watanabe, G. Bronner, M. H. Abraham and K.-U. Goss, UFZ-LSER database, v 3.2.1, http://www.ufz.de/lserd, (accessed February 17, 2022).

44 S. H. Hilal, S. W. Karickhoff and L. A. Carreira, *Verification and Validation of the SPARC Model*, EPA/600/R-03/033, 2003.

45 A. Klamt, F. Eckert and W. Arlt, COSMO-RS: An Alternative to Simulation for Calculating Thermodynamic Properties of Liquid Mixtures, *Annual Review of Chemical and Biomolecular Engineering*, 2010, **1**, 101–122.

46 A. J. Williams, C. M. Grulke, J. Edwards, A. D. McEachran, K. Mansouri, N. C. Baker, G. Patlewicz, I. Shah, J. F. Wambaugh, R. S. Judson and A. M. Richard, The CompTox Chemistry Dashboard: a community data resource for environmental chemistry, *Journal of Cheminformatics*, 2017, **9**, 61.

47 S. Kim, J. Chen, T. Cheng, A. Gindulyte, J. He, S. He, Q. Li, B. A. Shoemaker, P. A. Thiessen, B. Yu, L. Zaslavsky, J. Zhang and E. E. Bolton, PubChem in 2021: new data content and improved web interfaces, *Nucleic Acids Research*, 2021, **49**, D1388–D1395.

48 H. O. T. Pye, A. Nenes, B. Alexander, A. P. Ault, M. C. Barth, S. L. Clegg, J. L. Collett, K. M. Fahey, C. J. Hennigan, H. Herrmann, M. Kanakidou, J. T. Kelly, I. T. Ku, V. Faye McNeill, N. Riemer, T. Schaefer, G. Shi, A. Tilgner, J. T. Walker, T. Wang, R. Weber, J. Xing, R. A. Zaveri and A. Zuend, The acidity of atmospheric particles and clouds, *Atmospheric Chemistry and Physics*, 2020, **20**, 4809–4888.

49 E. Friese and A. Ebel, Temperature Dependent Thermodynamic Model of the System H+-NH4+-Na+-SO42--NO3--Cl--H2O, *The Journal of Physical Chemistry A*, 2010, **114**, 11595–11631.

50 A. S. Wexler and S. L. Clegg, Atmospheric aerosol models for systems including the ions H+, NH4+, N+, SO42−, NO3-, Cl-, Br-, and H2O, *Journal of Geophysical Research*, 2002, **107**, 4207.

51 Y. Tao and J. G. Murphy, Simple Framework to Quantify the Contributions from Different Factors Influencing Aerosol pH Based on NHx Phase-Partitioning Equilibrium, *Environmental Science & Technology*, 2021, **55**, 10310–10319.

52 A. Stenzel, K.-U. Goss and S. Endo, Experimental determination of polyparameter linear free energy relationship (pp-LFER) substance descriptors for pesticides and other

contaminants: New measurements and recommendations, *Environmental Science & Technology*, 2013, **47**, 14204–14214.

53 T. H. Nguyen, K.-U. Goss and W. P. Ball, Polyparameter linear free energy relationships for estimating the equilibrium partition of organic compounds between water and the natural organic matter in soils and sediments, *Environmental Science & Technology*, 2005, **39**, 913–924.

54 H. P. H. Arp, R. P. Schwarzenbach and K.-U. Goss, Ambient Gas/Particle Partitioning. 1. Sorption Mechanisms of Apolar, Polar, and Ionizable Organic Compounds, *Environmental Science & Technology*, 2008, **42**, 5541–5547.

55 H. P. H. Arp and K.-U. Goss, Ambient Gas/Particle Partitioning. 3. Estimating Partition Coefficients of Apolar, Polar, and Ionizable Organic Compounds by Their Molecular Structure, *Environmental Science & Technology*, 2009, **43**, 1923–1929.

56 Z. Wu, Y. Wang, T. Tan, Y. Zhu, M. Li, D. Shang, H. Wang, K. Lu, S. Guo, L. Zeng and Y. Zhang, Aerosol Liquid Water Driven by Anthropogenic Inorganic Salts: Implying Its Key Role in Haze Formation over the North China Plain, *Environmental Science & Technology Letters*, 2018, **5**, 160–166.

57 H. S. S. Ip, X. H. H. Huang and J. Z. Yu, Effective Henry's law constants of glyoxal, glyoxylic acid, and glycolic acid, *Geophysical Research Letters*, 2009, **36**, L01802.

58 X. Li, S. Song, W. Zhou, J. Hao, D. R. Worsnop and J. Jiang, Interactions between aerosol organic components and liquid water content during haze episodes in Beijing, *Atmospheric Chemistry and Physics*, 2019, **19**, 12163–12174.

59 Y. Moroi, H. Yano, O. Shibata and T. Yonemitsu, Determination of acidity constants of perfluoroalkanoic acids, *The Chemical Society of Japan*, 2001, **74**, 667–672.

60 D. A. Stewart and O. M. Essenwanger, A survey of fog and related optical propagation characteristics, *Reviews of Geophysics*, 1982, **20**, 481.

61 M. L. Brusseau, The influence of molecular structure on the adsorption of PFAS to fluid-fluid interfaces: Using QSPR to predict interfacial adsorption coefficients, *Water Research*, 2019, **152**, 148–158.

62 H. Xie, L. Feng, Q. Hu, Y. Zhu, H. Gao, Y. Gao and X. Yao, Concentration and size distribution of water-extracted dimethylaminium and trimethylaminium in atmospheric particles during nine campaigns - Implications for sources, phase states and formation pathways, *Science of The Total Environment*, 2018, **631–632**, 130–141.

63 S. K. R. Boreddy, P. Hegde and A. R. Aswini, Chemical Characteristics, Size Distributions, and Aerosol Liquid Water in Size-Resolved Coastal Urban Aerosols Allied with Distinct Air Masses over Tropical Peninsular India, *ACS Earth and Space Chemistry*, 2021, **5**, 457–473.

64 J. Cai, B. Chu, L. Yao, C. Yan, L. M. Heikkinen, F. Zheng, C. Li, X. Fan, S. Zhang, D. Yang, Y. Wang, T. v. Kokkonen, T. Chan, Y. Zhou, L. Dada, Y. Liu, H. He, P. Paasonen, J. T. Kujansuu, T. Petäjä, C. Mohr, J. Kangasluoma, F. Bianchi, Y. Sun, P. L. Croteau, D. R. Worsnop, V.-M. Kerminen, W. Du, M. Kulmala and K. R. Daellenbach, Size-segregated particle number and mass concentrations from different emission sources in urban Beijing, *Atmospheric Chemistry and Physics*, 2020, **20**, 12721–12740.

65 Q. Bian, X. H. H. Huang and J. Z. Yu, One-year observations of size distribution characteristics of major aerosol constituents at a coastal receptor site in Hong Kong – Part 1: Inorganic ions and oxalate, *Atmospheric Chemistry and Physics*, 2014, **14**, 9013–9027.

66 V. Bernardoni, M. Elser, G. Valli, S. Valentini, A. Bigi, P. Fermo, A. Piazzalunga and R. Vecchi, Size-segregated aerosol in a hot-spot pollution urban area: Chemical composition and three-way source apportionment, *Environmental Pollution*, 2017, **231**, 601–611.

67 K. Tamaki, Y. Ohara and S. Watanabe, Solution Properties of Sodium Perfluoroalkanoates. Heats of Solution, Viscosity *B* Coefficients, and Surface Tensions, *Bull Chem Soc Jpn*, 1989, **62**, 2497–2501.

68 N. Downes, G. A. Ottewill and R. H. Ottewill, An investigation of the behaviour of ammonium perfluoro-octanoate at the air/water interface in the absence and presence of salts, *Colloids and Surfaces A: Physicochemical and Engineering Aspects*, 1995, **102**, 203–211.

69 M. L. Brusseau and S. van Glubt, The influence of surfactant and solution composition on PFAS adsorption at fluid-fluid interfaces, *Water Research*, 2019, **161**, 17–26.

70 Y. Tian, Y. Yao, S. Chang, Z. Zhao, Y. Zhao, X. Yuan, F. Wu and H. Sun, Occurrence and phase distribution of neutral and ionizable per- and polyfluoroalkyl substances (PFASs) in the atmosphere and plant leaves around landfills: A case study in Tianjin, China, *Environmental Science and Technology*, 2018, **52**, 1301–1310.

71 N. Paragot, J. Bečanová, P. Karásková, R. Prokeš, J. Klánová, G. Lammel and C. Degrendele, Multi-year atmospheric concentrations of per- and polyfluoroalkyl substances (PFASs) at a background site in central Europe, *Environmental Pollution*, , DOI:10.1016/j.envpol.2020.114851.

72 E. Yamazaki, S. Taniyasu, X. Wang and N. Yamashita, Per- and polyfluoroalkyl substances in surface water, gas and particle in open ocean and coastal environment, *Chemosphere*, 2021, **272**, 129869.

73 S.-H. Seo, M.-H. Son, E.-S. Shin, S.-D. Choi and Y.-S. Chang, Matrix-specific distribution and compositional profiles of perfluoroalkyl substances (PFASs) in multimedia environments, *Journal of Hazardous Materials*, 2019, **364**, 19–27.

74 Y. Tao and J. G. Murphy, The sensitivity of PM2.5 acidity to meteorological parameters and chemical composition changes: 10-year records from six Canadian monitoring sites, *Atmospheric Chemistry and Physics*, 2019, **19**, 9309–9320.

75 Z. Meng, J. H. Seinfeld, P. Saxena and Y. P. Kim, Atmospheric Gas-Aerosol Equilibrium: IV. Thermodynamics of Carbonates, *Aerosol Science and Technology*, 1995, **23**, 131–154.

76 T. Ni, P. Li, B. Han, Z. Bai, X. Ding, Q. Wang, J. Huo and B. Lu, Spatial and Temporal Variation of Chemical Composition and Mass Closure of Ambient PM10 in Tianjin, China, *Aerosol and Air Quality Research*, 2013, **13**, 1832–1846.

77 P. Xiang, X. Zhou, J. Duan, J. Tan, K. He, C. Yuan, Y. Ma and Y. Zhang, Chemical characteristics of water-soluble organic compounds (WSOC) in PM2.5 in Beijing, China: 2011–2012, *Atmospheric Research*, 2017, **183**, 104–112.

78 E. H. Park, J. Heo, S. Hirakura, M. Hashizume, F. Deng, H. Kim and S.-M. Yi, Characteristics of PM2.5 and its chemical constituents in Beijing, Seoul, and Nagasaki, *Air Quality, Atmosphere & Health*, 2018, **11**, 1167–1178.

79 P. S. Zhao, F. Dong, D. He, X. J. Zhao, X. L. Zhang, W. Z. Zhang, Q. Yao and H. Y. Liu, Characteristics of concentrations and chemical compositions for PM2.5 in the region of Beijing, Tianjin, and Hebei, China, *Atmospheric Chemistry and Physics*, 2013, **13**, 4631–4644.

80 J. Ding, P. Zhao, J. Su, Q. Dong, X. Du and Y. Zhang, Aerosol pH and its driving factors in Beijing, *Atmospheric Chemistry and Physics*, 2019, **19**, 7939–7954.

81 B. Zhang, H. Shen, P. Liu, H. Guo, Y. Hu, Y. Chen, S. Xie, Z. Xi, T. N. Skipper and A. G. Russell, Significant contrasts in aerosol acidity between China and the United States, *Atmospheric Chemistry and Physics*, 2021, **21**, 8341–8356.

82 R. C. Sullivan, S. A. Guazzotti, D. A. Sodeman, Y. Tang, G. R. Carmichael and K. A. Prather, Mineral dust is a sink for chlorine in the marine boundary layer, *Atmospheric Environment*, 2007, **41**, 7166–7179.

83 H. M. Allen, D. C. Draper, B. R. Ayres, A. Ault, A. Bondy, S. Takahama, R. L. Modini, K. Baumann, E. Edgerton, C. Knote, A. Laskin, B. Wang and J. L. Fry, Influence of crustal dust and sea spray supermicron particle concentrations and acidity on inorganic NO₃[−] aerosol during the 2013 Southern Oxidant and Aerosol Study, *Atmospheric Chemistry and Physics*, 2015, **15**, 10669–10685.

84 H. Guo, A. Nenes and R. J. Weber, The underappreciated role of nonvolatile cations in aerosol ammonium-sulfate molar ratios, *Atmospheric Chemistry and Physics*, 2018, **18**, 17307–17323.

85 Y. Wang, L. Zhou, W. Wang and M. Ge, Heterogeneous Uptake of Formic Acid and Acetic Acid on Mineral Dust and Coal Fly Ash, *ACS Earth and Space Chemistry*, 2020, **4**, 202–210.

86 M. Guo, Y. Lyu, T. Xu, B. Yao, W. Song, M. Li, X. Yang, T. Cheng and X. Li, Particle size distribution and respiratory deposition estimates of airborne perfluoroalkyl acids during the haze period in the megacity of Shanghai, *Environmental Pollution*, 2018, **234**, 9–19.

87 K. Harada, S. Nakanishi, K. Sasaki, K. Furuyama, S. Nakayama, N. Saito, K. Yamakawa and A. Koizumi, Particle Size Distribution and Respiratory Deposition Estimates of Airborne Perfluorooctanoate and Perfluorooctanesulfonate in Kyoto Area, Japan, *Bulletin of Environmental Contamination and Toxicology*, 2006, **76**, 306–310.

88 H. Pickard, A. Criscitiello, C. Spencer, M. J. Sharp, D. C. G. Muir, A. O. de Silva and C. J. Young, Continuous non-marine inputs of per- and polyfluoroalkyl substances to the High Arctic: A multi-decadal depositional record, *Atmospheric Chemistry and Physics*, 2018, **18**, 5045–5058.

89 S. Lv, F. Wang, C. Wu, Y. Chen, S. Liu, S. Zhang, D. Li, W. Du, F. Zhang, H. Wang, C. Huang, Q. Fu, Y. Duan and G. Wang, Gas-to-Aerosol Phase Partitioning of Atmospheric Water-Soluble Organic Compounds at a Rural Site in China: An Enhancing Effect of NH_3 on SOA Formation, *Environmental Science & Technology*, 2022, **56**, 3915–3924.

90 R. Paris and K. v. Desboeufs, Effect of atmospheric organic complexation on iron-bearing dust solubility, *Atmospheric Chemistry and Physics*, 2013, **13**, 4895–4905.

91 V. Pratap, A. G. Carlton, A. E. Christiansen and C. J. Hennigan, Partitioning of Ambient Organic Gases to Inorganic Salt Solutions: Influence of Salt Identity, Ionic Strength, and pH, *Geophysical Research Letters*, , DOI:10.1029/2021GL095247.

92 Y. Tao and J. G. Murphy, The Mechanisms Responsible for the Interactions among Oxalate, pH, and Fe Dissolution in PM2.5, *ACS Earth and Space Chemistry*, 2019, **3**, 2259–2265.

93 J. Xu, J. Chen, Y. Shi, N. Zhao, X. Qin, G. Yu, J. Liu, Y. Lin, Q. Fu, R. J. Weber, S.-H. Lee, C. Deng and K. Huang, First Continuous Measurement of Gaseous and Particulate Formic Acid in a Suburban Area of East China: Seasonality and Gas–Particle Partitioning, *ACS Earth and Space Chemistry*, 2020, **4**, 157–167.

94 B. Stieger, D. van Pinxteren, A. Tilgner, G. Spindler, L. Poulain, A. Grüner, M. Wallasch and H. Herrmann, Strong Deviations from Thermodynamically Expected Phase Partitioning of Low-Molecular-Weight Organic Acids during One Year of Rural Measurements, *ACS Earth and Space Chemistry*, 2021, **5**, 500–515.

1